ACTIVE & REACTIVE POWERS CONTROL SCHEME FOR A GRID-CONNECTED PHOTOVOLTAIC GENERATION SYSTEM BASED ON VSI WITH SELECTIVE HARMONIC ELIMINATION

Ricardo L. Carletti [1], [3]
[1] Furnas Centrais Elétricas S.A.
Rua Real Grandeza, 219/613
Bloco B - Botafogo
22283-900 - Rio de Janeiro – RJ
carletti@furnas.com.br

Luis Claudio G. Lopes [2], [3]
[2] Centro Federal de Educação Tecnológica
Campus III – Leopoldina - MG
Rua José Peres, 558
36700–000 - Leopoldina – MG
gamboa@leopoldina.cefetmg.br

Pedro G. Barbosa [3]
[3] Universidade Federal de Juiz de Fora
Departamento de Energia Elétrica
Caixa Postal 422
36.001-970 - Juiz de Fora – MG
pedro.gomes@ufjf.edu.br

***Abstract* – This work presents an uncoupling active and reactive powers control strategy for DC-AC quasi-multipulse voltage source converters (VSC) to be used in a Dispersed Generation System (DGS) based on photovoltaic cells. The quasi-multipulse converters are switched using a selective harmonic elimination technique to minimize the voltage total harmonic distortion at the *point of common coupling* of the DGS. Digital simulation results, obtained with models developed for ATP/EMTP simulation package, and experimental measurements on a laboratory prototype will be used to verify the feasibility of the proposed method.**

Keywords – Dispersed Generation System, multipulse converter, programmed harmonic elimination-PWM.

I. INTRODUCTION

Nowadays, renewable energy sources based on photovoltaic cells (PV) have become a very attractive technology to generate extra amount of electrical energy in order to supply the increasing demand of the most industrialized countries [1]. There are some advantages that have been motivating grid-connected applications systems from few *Watts* to hundreds of *kilo-Watts*: (*i*) the reduction in the costs of the PV panels; (*ii*) the highly unlimited generation capability, due to its modularity and (*iii*) the fact of being emission-free [2].

A kind of classification based on the generation capacity of the photovoltaic grid-connected systems was proposed in [3], that is: (*i*) *small* – installed capacity of 1 to 10 *kilo-Watt-peak* (*kWp*); (*ii*) *medium* – from 10 *kWp* to hundreds of *kWp* and (*iii*) *large* – for applications with power ranging from 500 *kWp* to *MWp*, in centralized systems.

Fig. 1 shows a simplified schematic diagram of a photovoltaic grid-connected generation system. Static power converters (SPC) are used to transfer the electrical energy from the PV cells to an AC utility system. The DC-DC converter can optimize the performance of the PV cells through a maximum power point tracking (MPPT) algorithm that permits to extract maximum amount of power from the PV cells.

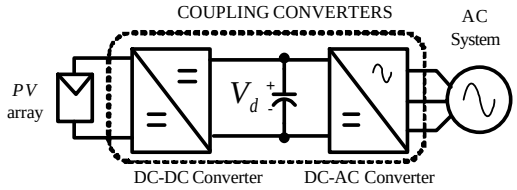

Fig. 1: Block diagram of a photovoltaic grid-connected generation system.

In this figure, the DC-AC converter injects the electrical energy that arrives in the DC link into the AC utility system. Nevertheless these equipments generate harmonics in its DC and AC terminals.

According to the previous classification, high-frequency PWM (Pulse Width Modulation) is generally used as the switching strategy of the DC-AC converter to reduce the harmonics in the output voltage of small capacity grid-connected systems. On the other hand, for large systems, it is advisable to turn on and off the semiconductors with a square-wave scheme, once the switching losses become critical. Regarding to the medium type, the authors have proposed in [4] a twelve-pulse voltage source converter (VSC) connection with a selective harmonic elimination switching strategy to reduce the harmonic on the converters terminals. This strategy employs a small number of six-pulse VSC and the equivalent switching frequency will be only seven times the industrial frequency, if a three-chop-per-half-cycle harmonic elimination technique is used. That keeps the switching losses on an acceptable level.

This work shows an algorithm to control the phase displacement of the output voltage of the grid-connected photovoltaic system with respect to the AC utility voltage and between the voltages of the two six-pulse VSCs. It will be shown that the active and the reactive powers can be controlled independently at the converter terminals. Digital simulation and experimental results obtained through the Alternative Transients Program (ATP/EMTP) and laboratory prototype will be used to investigate the performance and the feasibility of this control strategy.

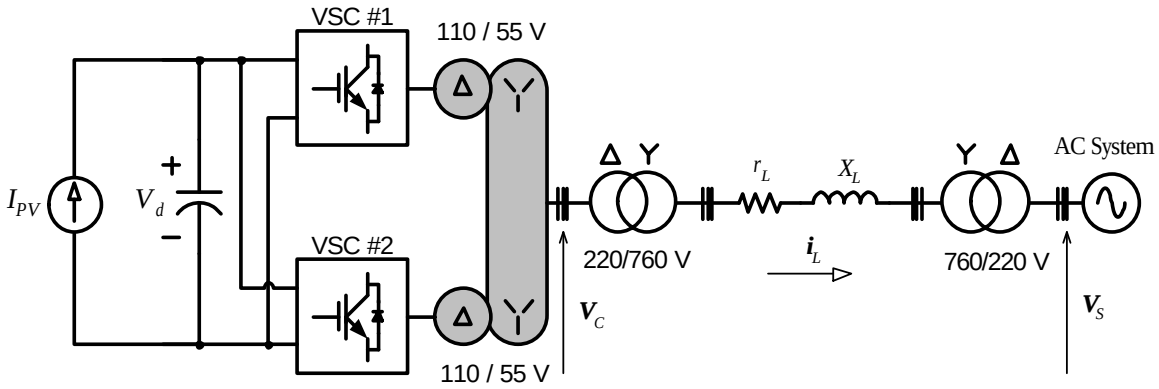

Fig. 2: Modeled dispersed generation system based on photovoltaic cells.

II. BASIC CONCEPTS

Fig. 2 shows the dispersed generation system studied in this work. The PV cells and the DC-DC converters were represented by a current controlled source. The DC-AC converter is formed by two three-phase VSCs that are connected in parallel on its DC side and in series on its AC side through six single-phase transformers.

The transformers turns-ratio shown in Fig. 2 were calculated in such a way that the loads near of the photovoltaic system, at the Campus of Federal University of Juiz de Fora, could be fed directly with distribution voltage levels (127 V / 220 V). However, the amount of the energy converted by the photovoltaic cells, which is not consumed, can be sent to a substation to feed other loads at the Campus. In this way, two transformer banks are used to increase and decrease the output voltage of the converters from 220 V to 760 V and again to 220 V in the substation in order to reduce the transmission losses.

Then, the phase-to-ground output *rms* voltage is calculated as follow, considering that each converter is switched using a selective harmonic elimination technique with three chops per half-cycle [4], [7] and [8].

$$V_C = \frac{1}{N}\left(\frac{4\sqrt{3}}{\pi}\right)V_d\left[1 - 2\cos\alpha_1 + 2\cos\alpha_2 - 2\cos\alpha_3\right]\cos\left(\frac{\gamma}{2}\right) \qquad (1)$$

where V_d is the DC-link voltage in (V); α_1, α_2 and α_3 are the angles in (*rad*) of the chops used to cancel the selected harmonics of the VSC output voltages, γ is the phase displacement angle between the two VSC output voltages in (*rad*) and N is the normalized transformer turns-ratio (N_1/N_2).

Nevertheless, since the converters of Fig. 2 are controlled to synthesize a set of three-phase voltages as given by (1), the phase-to-ground voltages at the PCC will have five different levels as shown in Fig. 3 (a). Fig. 3 (b) shows the harmonic spectrum of the simulated output voltage of the *quasi* 12-pulse VSC with selective harmonic elimination (VSC*q*12pHE). Note that the lower order harmonics are canceled similarly to what happens in the 18-pulse VSC. But here, this topology has the advantage of using only two converters.

In this figure, the angles α_1, α_2, α_3 and γ were made equals to 8.74°, 24.40°, 27.76° and 13.85°, respectively. These angles were calculated to cancel the 5th, 7th, 11th and 13th harmonics, respectively. The converter DC voltage is 178 V. Fig. 4 shows the output voltage of a $\pm 75\ kVA$ / 220 V *quasi* 12-pulse VSC with SHE. This result was obtained considering the converter without any load connected at its terminals and the VSC DC capacitor is 2000 μF.

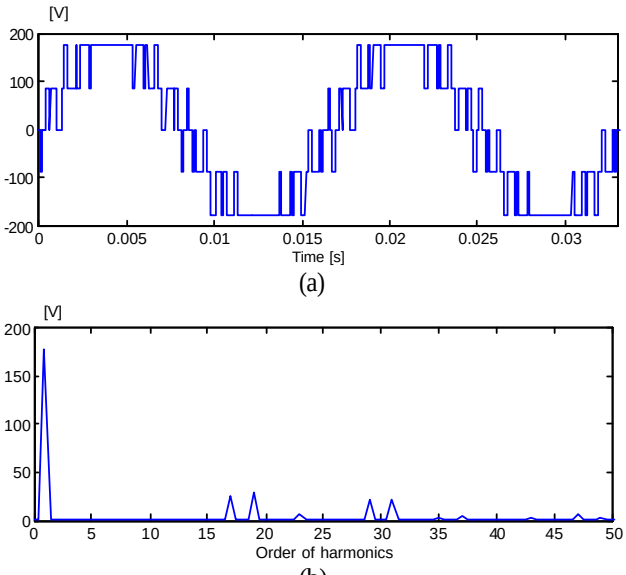

Fig. 3: Simulated results: (a) VSC output phase-to-ground voltage waveform with 3 notches per half-cycle; (b) harmonic spectrum.

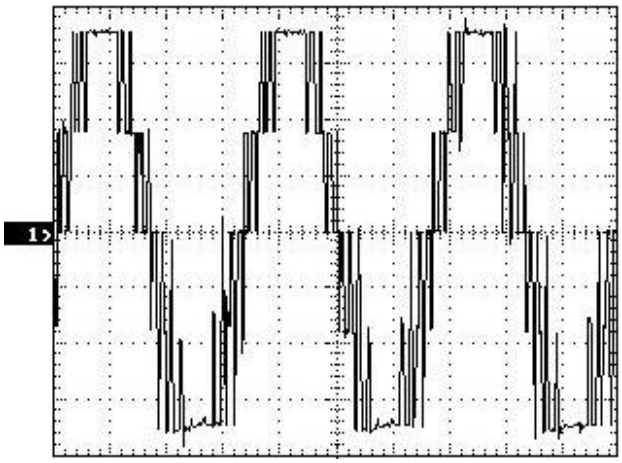

Fig. 4: Output phase-to-ground voltage waveform of a *quasi* 12-pulse VSC-SHE (vertical scale: 50 *V/div.*; horizontal scale: 5 *ms/div.*)

III. CONVERTER CONTROL ALGORITHM

Fig. 5 shows the phasor diagram of the studied photovoltaic grid-connected generation system. Neglecting the harmonics generated by the converters, from Fig. 5 and using (1), the active (P_C) and the reactive (Q_C) powers at the converter terminals are given by:

$$P_C = 3k\frac{V_S V_d}{X_L}\cos\left(\frac{\gamma}{2}\right)\sin\delta \qquad (2)$$

and

$$Q_C = 3\frac{V_S}{X_L}\left[V_S - kV_d\cos\left(\frac{\gamma}{2}\right)\cos\delta\right], \qquad (3)$$

where V_S is the *rms* utility voltage in (V), X_L is the equivalent reactance of the system and of the connection transformers in (Ω), δ is the phase displacement between the AC system voltage and the output converter voltage in (*rad*) and k is a constant obtained from (1) and given by $\left(2\sqrt{6}/\pi\right)N^{-1}\left[1-2\cos\alpha_1+2\cos\alpha_2-2\cos\alpha_3\right]$.

The analysis of sensibility of (2) and (3) shows that the angle δ is more effective to control the active power while the angle γ could be used to control the reactive power at the converter terminals. Thus, there is the possibility of controlling the phase displacement between the output voltages $V_{VSC\#1}$ and $V_{VSC\#2}$ to improve the controllability of the quasi twelve-pulse converter with selective harmonic elimination.

Fig. 6 shows the complete control diagram of the grid-connected photovoltaic generation system. The system output voltages and the line currents, after a α-β-0 transformation, are used to calculate the instantaneous imaginary power q_c [9]. This signal is compared to the reference value q^* and its error feeds a PI controller and its output is the phase-shifting angle γ between the two converter output voltages. A constant value γ_o is added to the phase-shifting angle γ in such a way to assure a symmetrical variation for the imaginary power, from its capacitive to inductive characteristic, at the converter terminals.

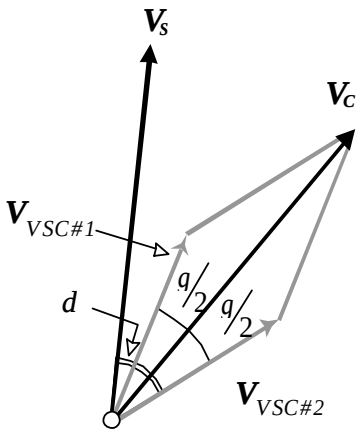

Fig. 5: Phasor diagram of grid-connected photovoltaic system.

On the other hand, the DC capacitor voltage increases when the PV cells inject more energy into the DC-link than the DC-AC converter transfers to the AC system and it decreases otherwise. In this way, the DC capacitor voltage could be used to control the active power injected by the converter into the AC system. Thus, the error signal between V_d and a reference value V_d^* feeds a PI controller which has the reference angle δ^* as output. This signal is proportional to the desired phase-shifted angle between the converter output voltage and the AC system voltage.

These angles and the AC system fundamental frequency (ω) and phase (ϕ), detected by a PLL circuit [5], are sent to the Phase Comparator Block to generate the turn-on and turn-off signals of the semiconductor switches. The Phase Comparator Block is also pre-programmed with the chops angles necessary to neutralize some harmonics of the output voltages.

IV. DIGITAL SIMULATION RESULTS

The *quasi* 12-pulse VSC with selective harmonic elimination switching was modeled using ATP/EMTP. Initially, the VSC*q*12pHE is in stand-by, that is, there is no real or imaginary powers flowing in the AC system.

Fig. 7 shows the phase "*a*" voltage and Fig. 8 shows the line current, both at the PCC (*Point of Common Coupling*). Fig. 9 shows the real instantaneous power and Fig. 10 shows the reference and measured imaginary instantaneous powers at the VSC*q*12pHE terminals. Finally, Fig. 11 exhibits the voltage at the DC-link capacitor.

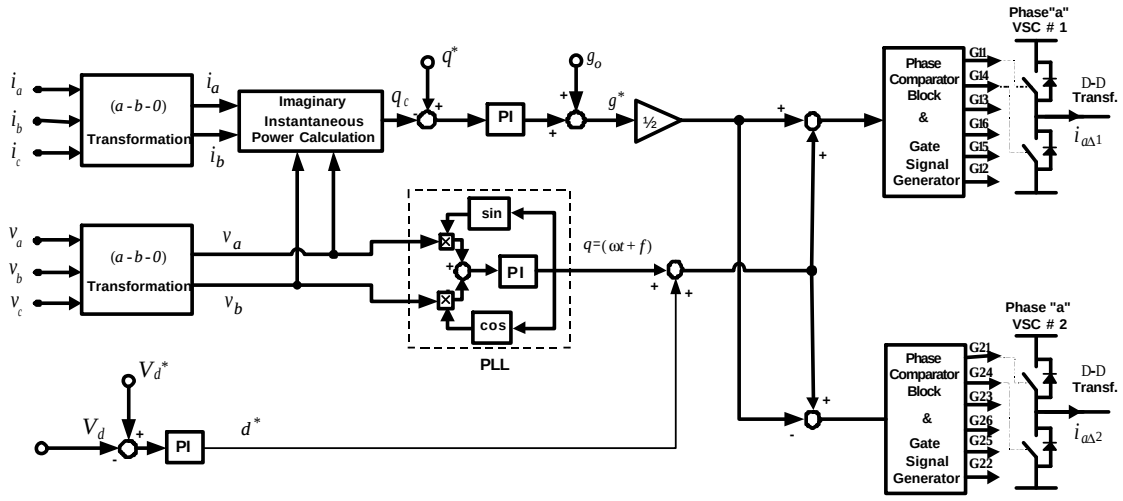

Fig. 6: DC-AC converter control diagram.

In $t = 0.05\ s$, the PV cells inject 25 kW in the DC-link capacitor. The DC-link capacitor voltage increases and the PI controller changes the reference angle δ^* to force the real power flow from the converter to the AC-system, discharging the capacitor. In $t = 0.30\ s$ the reference signal of the imaginary power q^* is step-changed from 0 to - 15 *kvai* (*kilo imaginary volt-ampere*). Then, the second PI controller is fed with a non-null error signal that changes the angle γ^* in a way to increase the magnitude of the converter output voltage and to synthesized the desired imaginary power at the converter terminals. In $t = 0.60\ s$, the power supplied by the PV panels drops to 20 kW, and the DC capacitor voltage decreases. Then, the PI controller changes the angle δ^* in order to hold the DC voltage at the reference value $V_d^* = 178\ V$.

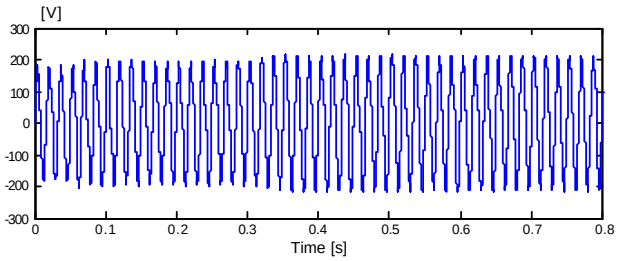

Fig. 7: Phase '*a*' DGS voltage at PCC

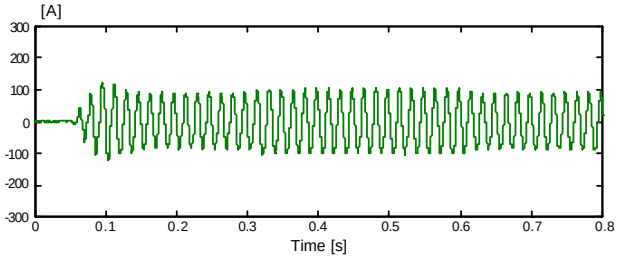

Fig. 8: Phase '*a*' line current at PCC

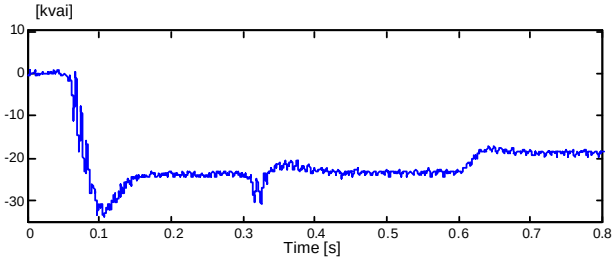

Fig. 9: Real power at VSC *q*12pHE terminals.

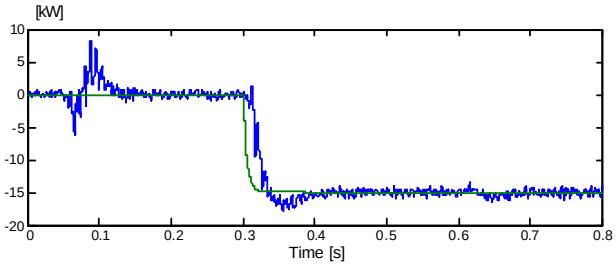

Fig. 10: Imaginary power at VSC *q*12pHE terminals.

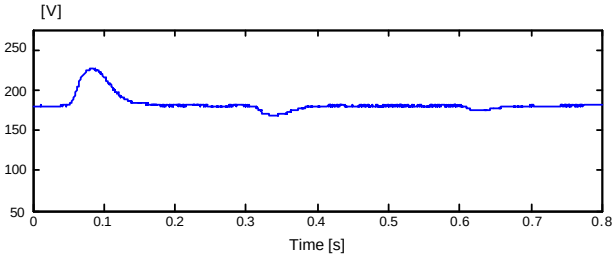

Fig. 11: DC-link converter voltage.

As shown above, the behavior of the imaginary power at the converter terminals can be controlled "*independently*" of the value of the converter DC voltage. This characteristic makes it possible to use the reference DC voltage as a fine tune for improving a MPPT

(*Maximum Power Point Tracking*) algorithm to extract the maximum amount of real power from the PV cells.

V. EXPERIMENTAL RESULTS

The good results obtained with the digital simulation model guided us to the practical implementation of the dispersed generation system presented in this work starting from the topology shown in the Fig. 2. The converters, connected through single-phase transformer banks, are switched with a programmed harmonic elimination scheme. They are based on Semikron IGBT switches and have an equivalent capacitor of $2000\,\mu F/350\ V$ connected at their DC terminals. Fig. 12 shows a picture of one VSC and its single-phase transformer bank. These transformers have their coils connected in Δ on the side of the converters and in open-Y on the other side. This scheme allows the voltages generated by one VSC to be added to the voltages generated by the other VSC to generate three-phase output voltages similar to that shown in the Fig. 4.

Fig. 12: Picture of one VSC and its transformers bank.

The control algorithm shown in Fig. 6 and tested with ATP/EMTP was implemented into a fixed-point TMS320F243 DSP (*Texas Instruments Digital Signal Processors*) with a clock frequency of 20 *MHz*. However to improve the performance of the control algorithm the tasks were split between three DSPs as shown in Fig. 13. Each converter is controlled by an independent DSP that is programmed with the harmonic elimination angles given by (1) and with a phase comparator algorithm. The phase comparator is responsible for generating the pulses to turn-on and turn-off the IGBTs. Each VSC DSP has also an algorithm to detect the system frequency and phase (PLL) [5].

The three-phase voltages and currents are sampled by the third DSP that are programmed with the imaginary and DC voltage control loops.

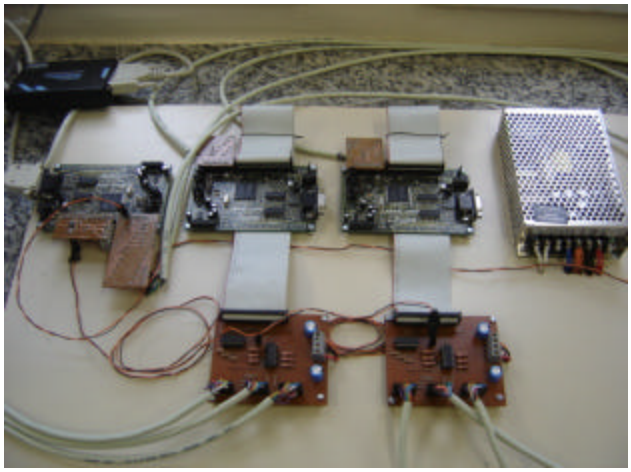

Fig. 13: Picture with the DSPs.

Fig. 14 shows the phase "*a*" system voltage waveform after the connection of the converters at the PCC (*Point of Common Coupling*) while Fig. 15 shows the current inject in phase "*a*" of the system. Note that there are some notches in the system voltage. However the converters are connected directly to the AC system through their transformer banks and without any passive filter at their output terminals. The voltage and current waveforms could be improved by using small capacitors as output filters and/or increasing the number of chops in the selective harmonic technique. However these options will not be investigated in this work.

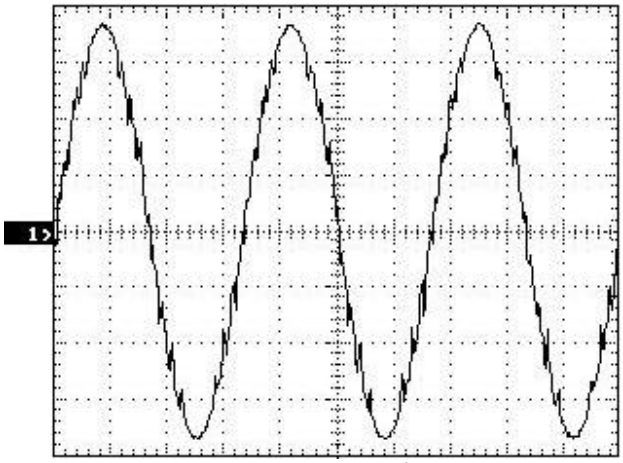

Fig. 14: DGS output voltage waveform at the PCC (vertical scale: 50 *V/div.*; horizontal scale: 5 *ms/div.*)

VI. CONCLUSIONS

This work described some basic concepts and principles of operation of a DC-AC converter as a dispersed generation system based on photovoltaic cells. The uncoupled control of the active and reactive powers gives to this DGS flexibility and operational advantages and it assures the quality of the voltage generated with a low number of pulses per cycle. The 12-pulse VSC with

selective harmonic elimination technique improves the output voltage waveform spectrum. The proposed control scheme and the harmonic elimination technique can be used for VSC with large number of pulses. The ATP/EMTP and laboratory prototype were used to model and illustrate the operation of the DGS.

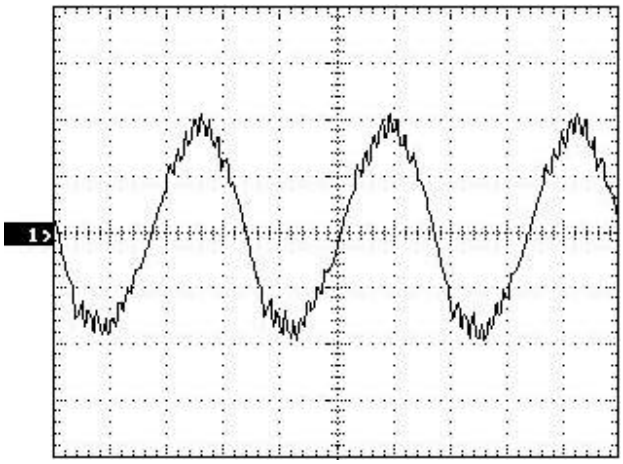

Fig. 15: Line current at the PCC (vertical scale: 50 *A/div.*; horizontal scale: 5 *ms/div.*)

VII. REFERENCES

[1] A. Sayigh, "World Renewable Energy", *in Third World Conference on Photovoltaic Energy Conversion*, Oral Plenary, May 2003, pp. 2560-2561.

[2] R. Ramakumar et al, "Renewable Technologies and Distribution Systems", IEEE Power Engineering Review, Vol. 19, No. 11, Nov. 1999, pp. 5-14.

[3] L. Castañer and S. Silvestre, "Modelling Photovoltaic Systems" , John Wiley and Sons, 2002

[4] R. L. Carletti, L. C. G. Lopes and P.G. Barbosa, "A Dispersed Generation System Based on Photovoltaic Cells: Converter Configuration and Switching Strategy", *in Proc. of VII Brazilian Power Electronics Conf.* - COBEP, Fortaleza, Brazil, September 2003, pp. 404-409.

[5] L. C. G. Lopes, R. L. Carletti and P.G. Barbosa, "Implementation of a Digital and a Deadbeat PLL Circuit Based on Instantaneous Power Theory with DSP TMS320F243", *in Proc. of VII Brazilian Power Electronics Conf.* - COBEP, Fortaleza, Brazil, September 2003, pp. 404-409.

[6] P.G. Barbosa, C.A.C. Cavaliere e E.H. Watanabe et al, "Topologia de um STATCOM para Sistemas de Distrubuição Baseado na Conexão Série de Conversores VSI *Quasi* Multipulso", *in Anais do Congresso Brasileiro de Automática* - CBA, Natal, RN, 2002.

[7] N. Mohan et al. al, "Power Electronics: Converters, Applications and Design", John Wiley and Sons, 2nd edition, 1994.

[8] Y.H. Song and A.T. Johns, "Flexible AC Transmission Systems (FACTS)", IEE Power Engineering Series, 1999.

[9] E.H. Watanabe, M. Aredes, "Teoria de Potência Ativa e Reativa Instantânea e Aplicações – Filtros Ativos e FACTS", *in Congresso Brasileiro de Automática* - CBA'98, Uberlândia, Brasil, Setembro 14-18, 1998.